

The equivalence between Eq. (A.1) and the one-body form of Eq. (A.2) may easily be displayed. This equivalence does not carry over to the present problem, however. If there exist solutions of the associated eigenvalue equation with energies in the continuum, which decay asymptotically, these solutions satisfy Eq. (A.2) but not Eqs. (2.9). They would be required for completeness but would not be included if the boundary conditions given by Eqs. (2.9) are adopted. A calculation of α_θ and β_θ would have to take into account the additional bound state solutions, thereby possibly complicating the problem considerably. We note, however, that if these additional solutions are orthogonal to the function we are expanding (i.e., the difference function w) their omission is of no consequence in an application of the Kato method.

Now bound-state solutions embedded in the con-

tinuum exist by virtue of their belonging to a different symmetry class from the scattering solutions and consequently being orthogonal to them. If the trial function is chosen with the correct symmetry properties then w will be orthogonal to the additional decaying solutions. Difficulties may arise if the true scattering solution has symmetry properties which are not easily recognizable. (Such difficulties are of course not peculiar to the Kato method; they exist for the ordinary variational principle as well.) We do not believe that any hidden symmetries exist in the e^+H problem. In any event, as we have already noted, we are able to claim complete rigor for the bound we have obtained on the e^+H scattering length, aside from any questions of completeness, by virtue of our having given an independent proof of the validity of the bound.

Measurement of the Total, Differential, and Exchange Cross Sections for the Scattering of Low-Energy Electrons by Potassium*†

KENNETH RUBIN,‡ JULIUS PEREL, AND BENJAMIN BEDERSON

Department of Physics, New York University, University Heights, New York, New York

(Received July 9, 1959)

An atom beam recoil technique has been used to determine the total, Q , differential, $\sigma(\theta)$, and differential exchange, $\sigma_e(\theta)$, cross sections for the scattering of low-energy electrons by potassium. The method consists of observing the angular distribution of atoms scattered from a potassium atom beam which has been cross fired by an electron beam. Relative values of $\sigma(\theta)$ are then obtained by transforming to electron scattering angles. An inhomogeneous magnet and collimating channel are used as a velocity filter for the atom beam. Curves representing the variation of $\sigma(\theta)$ with θ between approximately 15° and 60° are

presented for various electron energies between 0.6 and 9.0 ev.

The magnet also serves to polarize the beam. Relative values of $\sigma_e(\theta)$ were determined by observing the amount of depolarization of the beam in the scattering region, using a second inhomogeneous magnet as an analyzer. Over the observed range of angles, exchange accounts for approximately one third of the scattering. Bounds on the total exchange cross section, Q_e , are also tabulated for energies between 0.5 and 4.0 ev. The bounds on Q_e at 0.5 volt are $0.8 \times 10^{-14} \text{ cm}^2 < Q_e < 1.6 \times 10^{-14} \text{ cm}^2$.

1. INTRODUCTION

THE exchange interaction during an electron-atom scattering event plays a significant role in many scattering processes. Such interactions, however, have not been extensively studied. In some recent experiments performed by Dehmelt,¹ Novick and Peters,² and Franken *et al.*,³ bounds on the cross sections for exchange scattering of thermal electrons by alkali atoms have been obtained. In these experiments, exchange cross sections were determined by observing depolarization by free electrons of an alkali gas previously aligned by optical pumping.

The main purpose of the present experiment was to observe exchange events directly by cross firing a polarized atom beam with a monoenergetic electron beam. Exchange collisions result in a readily observable partial depolarization of the atom beam. The method thus makes it possible to study exchange scattering as a function of electron energy. Furthermore, because of the recoil suffered by scattered atoms, these can readily be distinguished from the unscattered atom beam.^{4,5} It is, therefore, possible to investigate differential scattering by observing the angular distribution of the scattered atoms.

By the use of this method, we have determined relative values of the differential cross section $\sigma(\theta)$ and the differential exchange cross section $\sigma_e(\theta)$ for the scattering of potassium by electrons over a range of

* Supported by the Office of Naval Research.

† For preliminary reports of this work, see Bull. Am. Phys. Soc. **2**, 270 (1957) and Bull. Am. Phys. Soc. **4**, 234 (1959).

‡ From part of a thesis submitted by K. Rubin in partial fulfillment of the requirements for the degree of Doctor of Philosophy, Department of Physics, New York University.

¹ H. G. Dehmelt, Phys. Rev. **109**, 381 (1958).

² R. Novick and H. E. Peters, Phys. Rev. Letters **1**, 54 (1958).

³ Franken, Sands, and Hobart, Phys. Rev. Letters **1**, 52 (1958).

⁴ W. E. Lamb and R. C. Retherford, Phys. Rev. **79**, 549 (1950).

⁵ Rubin, Perel, and Bederson, New York University Technical Report No. 1, Nonr 285(15), 1957 (unpublished).

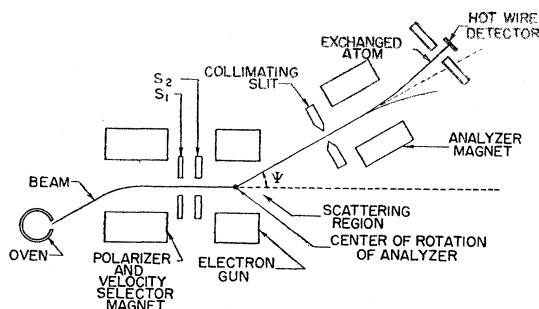


FIG. 1. Schematic diagram of the apparatus.

electron polar scattering angles θ , as well as over a range of electron energies. From the measured values of $\sigma_e(\theta)$, bounds are then made on the total exchange cross section Q_e .

2. OUTLINE OF METHOD

An atom beam of potassium is both polarized and analyzed by passing it through inhomogeneous magnetic fields.⁶ If an exchange event occurs with a cross-fired electron whose spin is oriented opposite to the spin of the atomic valence electron, the atom reverses its polarization state. This assumes that the atom's polarization is due solely to the spin orientation of the valence electron, and not to the nuclear spin system. In the present experiment a field of about 1000 gauss in the scattering region serves to decouple the nuclear and atomic spin systems, satisfying the above requirement.⁷ Exchange collisions due to electrons whose spins are parallel to the valence electron are, of course, unobservable.

The arrangement of the apparatus for the exchange experiment is shown in Fig. 1. The potassium oven is offset from the axis of the polarizing magnet so that only those atoms which are bent back towards the axis by a definite amount can pass through the collimating slits S_1 and S_2 , giving a polarized and velocity filtered atom beam.⁸ Velocity selection is necessary if one wishes to calculate an equivalent electron scattering angle θ from an observed atom scattering angle ψ . The relation between θ and ψ as a function of atom and electron velocities is discussed in Sec. 5.

Because of the spread of the recoil angles of the scattered atoms, it is necessary to rotate both the analyzer magnet and detector about the scattering region. With the magnet and detector set at some angle ψ with respect to the beam axis, as shown in Fig. 1, and with no current in the analyzer magnet windings,

⁶ N. F. Ramsey, *Molecular Beams* (Oxford University Press, New York, 1956), p. 399 ff.

⁷ To be certain that an exchange event is the only process which can change the polarization state of the atom, the magnetic interaction of the free electron-atom system must be small. It can be readily shown that this is indeed the case.

⁸ An analysis of the use of an inhomogeneous magnet and slit system as a velocity filter will be given in a forthcoming New York University technical report.

the signal at the detector represents the total number of atoms scattered between the angles ψ and $\psi + \Delta\psi$, where ψ is the angle subtended by the atom beam detector at the scattering center. This signal is therefore a measure of the differential scattering at the angle ψ averaged over $\Delta\psi$. If current is now passed through the analyzer magnet windings, the scattered beam will split into two components. The ratio of the number of atoms in each spin state may be measured by first moving the detector to one side of the magnet axis and then the other. The method of obtaining $\sigma_e(\theta)/\sigma(\theta)$ from this data is discussed in Sec. 5(b).

Total cross-section measurements are made by setting the analyzer magnet (no current) and atom detector on the axis of the unscattered atom beam and measuring the change in atom signal when the electron beam is turned on.

3. APPARATUS

The vacuum envelope is divided into a source chamber and a main chamber, which are separated by a bulkhead containing a beam shutter. Normal operating pressures are 5×10^{-6} mm Hg and 3×10^{-7} mm Hg in the source and main chambers, respectively. The source is a conventional K oven,⁹ operating at a temperature of 300°C , and has a slit 0.003 in. wide and 0.5 in. high. To facilitate taking the differential and exchange data the analyzer and the detector are capable of being driven automatically and independently.

Magnets

The polarizing and analyzing magnets are identical and have pole faces corresponding to equipotentials of an equivalent two wire system. The calculated ratio of field gradient to field for both magnets is 5 cm^{-1} . Each magnet is 4 in. long.

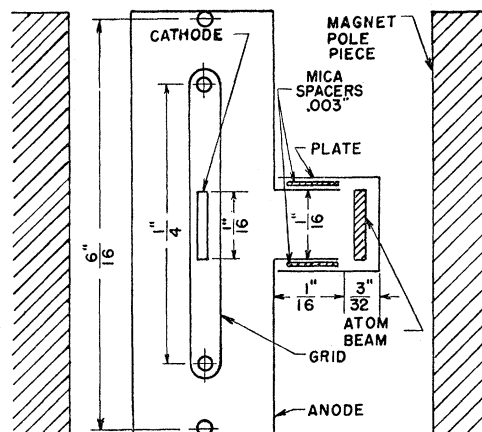


FIG. 2. Cross section of the electron gun.

⁹ N. F. Ramsey, *Molecular Beams* (Oxford University Press, New York, 1956), p. 364 ff.

Electron Gun

A cross section of the electron gun is shown in Fig. 2. The cathode, grid, and mica spacers are parts of a Sylvania 6L6 tube assembly. The plate is shaped in the form of a channel 1 in. long, and is insulated from the anode. (The plate current passes through the atom beam and is responsible for the scattering.) The gun is mounted so that the atom beam (seen end on in the diagram) enters the gun close to the end of the anode channel so that the scattering occurs in an equipotential region. Anode and plate are maintained at the same potential. The strong magnetic field which serves to decouple the nuclear and atomic spin systems also serves to confine the electron beam.

The plate current is varied by adjusting the grid voltage while the electron energy is varied by adjusting the potential between the cathode and anode. The true value of the electron energy is obtained by measuring the plate current as a function of a retarding potential placed between plate and anode. The retarding potential measurements indicate that nominal voltage readings over the range studied must be reduced by approximately one volt and this correction has been applied to all quoted voltages. Similar measurements were made to determine the energy spread in the electron beam. The spread is about 0.5 volt over the entire energy range.

Detection System

The detector is of the conventional surface ionization type. It consists of a length of 10-mil platinum wire mounted in the center of a brass cylinder which contains an opening for the beam.

An ac modulating and detecting system is employed in order to minimize noise due to fluctuations in the atom beam as well as in the hot wire background. The current in the electron gun is modulated by applying a 30-cps voltage to the grid, resulting in a 30-cps scattering signal at the detector. This signal is fed into a narrow band, phase sensitive amplifier. In the present experiment, scattering out of the detector produces a positive output signal; scattering into the detector produces a negative output signal. A block diagram of the detection system is shown in Fig. 3. The total dc beam at any detector position can be measured by an electrometer circuit.

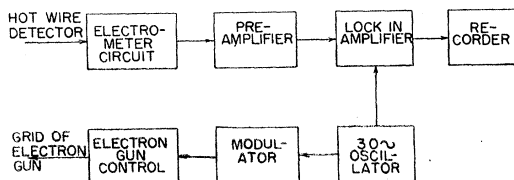


FIG. 3. Block diagram of the detection system.

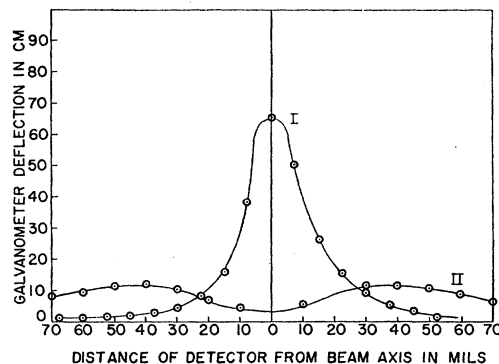


FIG. 4. I. dc beam shape with polarizer and analyzer magnets off. II. dc beam shape with polarizer magnet off and analyzer magnet on.

4. DATA

The data are arranged in two categories, dc measurements and ac measurements. (The analysis of the data is left for the next section.)

Direct Current Measurements

The dc measurements refer to the atom beam intensity data taken with the electron gun off, and were taken to study the beam characteristics. The data are presented in Figs. 4 and 5 in the form of graphs of relative beam intensity *vs* transverse displacement of the detector from the beam axis, for various combinations of the polarizer and analyzer magnets on and off. The ordinate units are the same in both figures. Curve I of Fig. 4 represents data taken with both magnets off, while curve II of Fig. 4 represents data taken with the analyzer magnet on and the polarizer magnet off. Curve I of Fig. 5 represents data taken with the polarizer magnet on and analyzer magnet off while curve II of Fig. 5 represents data taken with both magnets on. Note that whenever the polarizer magnet is on, the oven has been offset from its center position. The optimum displacement of the oven is determined by observing the beam intensity as the

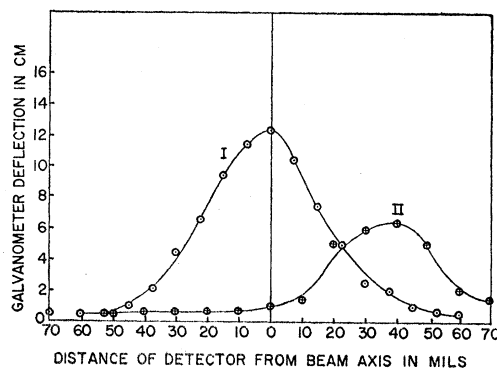


FIG. 5. I. dc beam shape with polarizer magnet on and analyzer magnet off. II. dc beam shape with polarizer and analyzer magnets on.

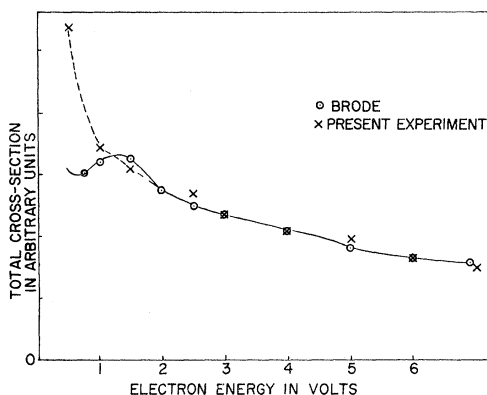


FIG. 6. Total cross section in arbitrary units as a function of electron energy. The solid curve represents Brode's results. The present data are normalized to Brode's data at 4 volts.

oven is moved. When the oven is at a position for which the beam intensity assumes its maximum value (one on each side of the beam axis), the atom beam emerging from the channel possesses a narrow distribution of velocities centered about the most probable beam velocity.

Alternating Current Measurements

The ac measurements refer to the signals observed with the ac detection system, and therefore represent scattering signals. Three different kinds of scattering data were taken: total, differential, and exchange, and the procedure for obtaining each kind is now described.

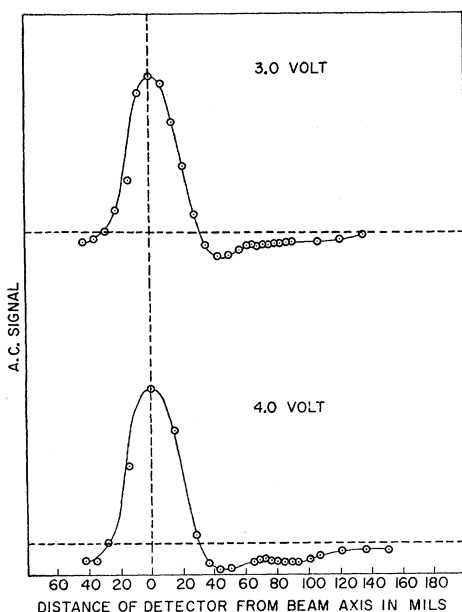


FIG. 7. Sample differential scattering curves, taken at 3.0 and 4.0 volts. The curves represent scattered atom current in arbitrary units as a function of atom detector position. Direction of momentum transfer is to the right.

(a) Total Cross-Section Data

The total cross-section data were taken with the detector fixed on the beam axis. The data thus obtained are presented in Fig. 6, and include a comparison with the data of Brode,¹⁰ which are normalized to our data at four volts. Because of the higher energy resolution in Brode's experiment, we have plotted average values of his original data over 0.5-volt intervals. It is seen that the comparison is quite satisfactory over most of the energy range. At very low energies (<1 volt) our total cross-section values increase quite rapidly with decreasing energy, and work is presently in progress to investigate this energy region in more detail.

(b) Differential Cross-Section Data

A sample of the differential scattering data at 3 and 4 volts, obtained by recording the ac signal as a function of ψ (with velocity selection), is presented in Fig. 7. Data taken at 1 volt both with and without velocity selection are presented in Fig. 8.¹¹ The small negative

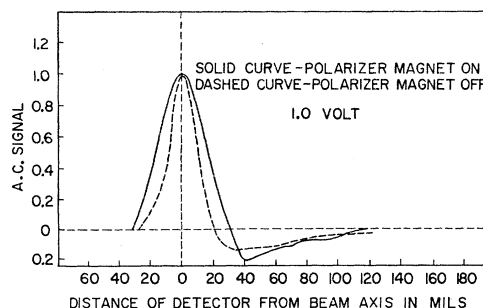


FIG. 8. The effect of the velocity selector on the differential scattering curves.

peaks at 70 and 90 mils are absent in the latter curve, due to the smearing effect of the velocity distribution. The difference in width of the positive portions of the two curves is due to the broadening of the beam by the polarizer, as will be explained in Sec. 5.

(c) Exchange Cross-Section Data

The exchange data are obtained by setting the analyzer magnet axis at a particular value of ψ . With the polarizer and analyzer magnets on, the detector is then traversed from one side of the analyzer magnet axis to the other (generally done automatically). Samples of data obtained in this manner are shown in Fig. 9 for two angles at a number of electron energies. The peak labelled *E* represents the exchange signal in each case. We define $R(\psi)$ as the ratio of the amplitudes of the principal peak to the exchange peak. Column III

¹⁰ R. B. Brode, Phys. Rev. **34**, 673 (1929).

¹¹ In Figs. 7 and 8, displacement of the detector from the beam axis is given in mils (0.001 in.). The detector is 14 in. from the scattering center so that ψ in radians may be obtained by dividing the displacement in mils by 14 000.

of Table I gives $R(\psi)$ for various electron energies (Column I) and scattering angles (Column II).

Although the exchange data in this paper are restricted to elastic scattering, Fig. 10(a), illustrating the angular dependence of the exchange scattering at 12 volts, is included for interest. It was taken by recording the maximum of the exchange peak as a function of ψ . A comparable curve at lower electron energy would be difficult to obtain because of the unfavorable signal to noise ratio. Figure 10(b) was obtained by recording the maximum of the principal peak as a function of ψ , also at 12 volts.

TABLE I. Summary of exchange results. Column I, Electron energy in volts; Column IIa, atomic scattering angle ψ in 10^{-3} radian; Column IIb, corresponding electron scattering angle θ in degrees; Column III, the observed ratio of the two polarization peaks at ψ , $R(\psi)$; Column IV, the ratio $\sigma_e(\theta)/\sigma(\theta)$; Column V, scattering signal at ψ in arbitrary units; Column VI, exchange signal at ψ , in the same arbitrary units as Column V; Column VII, the estimated ratio $\int_{\theta_{\min}}^{\theta_{\max}} \sigma_e(\theta) d\theta / \int_{\theta_{\min}}^{\theta_{\max}} \sigma(\theta) d\theta$; Column VIII, the lower bound on Q_e/Q ; Column IX, the upper bound on Q_e/Q ; Column X, upper and lower bounds in units of 10^{-14} cm² (using Brode's absolute values for Q).

I	IIa	IIb	III	IV	V	VI	VII	VIII	IX	X
0.5	3.5	47	5.6	0.16	7.5	1.2				
	6.3	69	2.7	0.46	4.5	2.1	0.35	0.20	0.40	$0.87 < Q_e < 1.6$
	8.8	84	2.0	0.62	2.5	1.5				
1.0	3.5	42	5.9	0.14	8.5	1.2				
	6.3	56	3.0	0.41	5.0	2.1	0.27	0.12	0.32	$0.55 < Q_e < 1.5$
	8.8	68	2.8	0.44	2.0	0.9				
2.0	3.5	35	6.5	0.11	12.5	1.4				
	4.3	38	5.1	0.19	11.0	2.1				
	5.0	42	4.5	0.24	8.0	1.9	0.30	0.14	0.50	$0.56 < Q_e < 2.0$
3.0	6.3	47	2.7	0.46	5.5	2.5				
	8.8	56	1.9	0.63	3.0	1.9				
	3.5	32	5.9	0.14	9.0	1.3				
4.0	5.0	38	4.6	0.23	6.5	1.5	0.30	0.13	0.57	$0.45 < Q_e < 2.0$
	6.3	43	2.6	0.48	5.0	2.4				
	8.8	51	2.2	0.57	2.8	1.6				
4.0	3.5	30	3.7	0.32	8.0	2.6				
	5.0	35	5.8	0.15	6.5	1.0	0.25	0.11	0.57	$0.33 < Q_e < 1.7$
	8.8	47	4.5	0.24	4.5	1.1				

5. ANALYSIS OF DATA

Direct Current Measurements

Curve II of Fig. 5 shows that the beam is at least 90% in one polarization state. This can be seen by comparing the signals at 0.040 in. to the left and right of the beam axis. The ratio of these signals is always greater than 10 to 1.¹²

A comparison of curves I of Figs. 4 and 5 reveals that the polarizer magnet and channel produces a significant broadening of the beam. This is to be expected since the velocity dependence of the deflection in the polarizing magnet causes a spread in the beam equivalent to that which would be obtained by an effective source placed directly in front of S_1 of Fig. 1. The calculated

¹² The curves of Fig. 10 also indicate that the beam is 90% polarized, since the positive (scattering out) signal of Fig. 10(a) must be attributed to residual atoms of the unwanted spin state. The peak of this positive signal is approximately $\frac{1}{10}$ of the peak of the positive signal of Fig. 10(b).

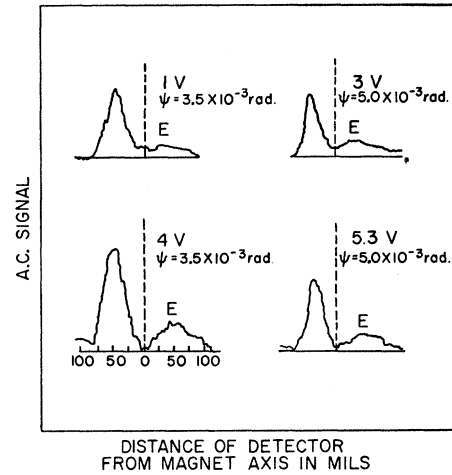


FIG. 9. Samples of exchange data taken automatically. The peak labelled E represents signal due to scattered atoms which have changed their spin state.

beam shape, assuming that the source is directly in front of S_1 , does in fact yield a beam shape in good agreement with that of curve I of Fig. 5.

The effectiveness of the velocity filter is demonstrated by comparing the beam shapes of the deflected to the undeflected beam in Fig. 5. The analyzer produces essentially no change in the beam shape, in sharp contrast to the broadening produced by the analyzer as shown by curve II of Fig. 4, in which there was a normal velocity distribution. (The smaller amplitude of curve II, relative to curve I, of Fig. 5 is due to the collimating slit in front of the analyzer magnet.)

Alternate Current Measurements

(a) Differential Scattering Data

We first make some general remarks concerning the curves of Figs. 7 and 8. If the detector were capable of traveling sufficiently far off the beam axis so as to collect all the scattered atoms, the areas under the positive and negative parts of the curves should be equal. In actual fact the range of motion of the detector

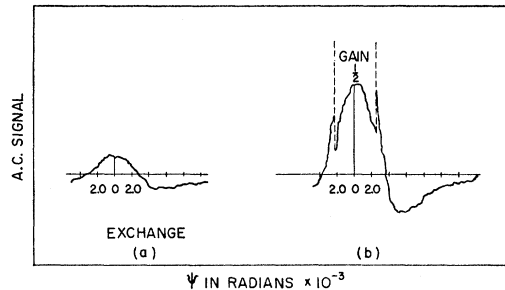


FIG. 10. Curve (a): recording of the maximum of the exchange peak as a function of atom scattering angle ψ . Curve (b): recording of the maximum of the principal peak as a function of ψ . Electron energy is 12 volts in both curves.

was limited to about 0.30 in. off the axis, because of the interference of the vacuum envelope. Such a maximum displacement would collect all atoms scattered by 0.5-volt electrons. For higher energies, some of the scattered beam cannot be collected, with the result that the negative areas are always smaller than the positive ones, with the ratio of the two areas decreasing as the energy increases. This limitation on detector travel is the principal cause of error in the determination of Q_e , as will be seen later.

In order to analyze the data we must take into account the finite width of the potassium beam. Part of the observed scattering signal lies within the region of the dc beam. At any point within this region, the scattering signal is actually the algebraic sum of two signals of opposite sign, one caused by scattering out of the beam at the position of the detector (positive), and the other caused by scattering into the detector from other portions of the beam (negative). It is possible to correct for the finite dc beam width to obtain angular distributions for angles which are smaller than the angle subtended by the dc beam itself. This can be accomplished in the following manner.

If there were no scattering in, the ac signal would follow the dc beam shape exactly, since the scattering out signal at any detector position is proportional to the total beam current at that position. A theoretical scattering out curve can thus be calculated from the dc beam shape by multiplying the dc signal at each detector position by a constant factor which depends upon Q , the electron current density, and the over-all gain of the ac detection system. This theoretical scattering out curve can now be plotted together with the observed ac scattering data. At each detector position, the difference between the amplitudes of the two curves represents the amount of scattering into the detector at that position from other portions of the dc beam.

An idealized situation is presented in Fig. 11. Curve *A* represents the dc beam intensity (not drawn to scale), as a function of detector position, y . We take $y=0$ at the left edge of the beam. Curve *B* represents the scattering out curve, which is proportional to curve *A*. Curve *C* represents the observed scattering signals. Curve *D* represents $C-B$, that is, the scattering in signal alone. We now wish to relate the scattering in signals, as represented in curve *D*, to the differential cross sections.

If y' is the lateral displacement of a scattered atom along the line of motion of the detector and $p(y')dy'$ is the probability of an atom being scattered into the range dy' at y' , then the total probability of an atom being scattered is given by

$$P_a = \int_0^{y_{\max}'} p(y')dy' = j_e Q a / V e, \quad (1)$$

where j_e is the electron current density, a the path

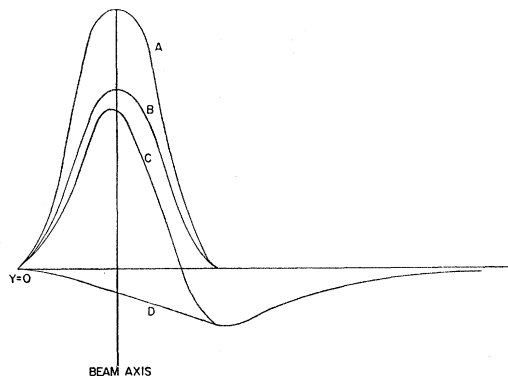


Fig. 11. An idealized set of curves representing A: dc beam shape, B: scattering out signal, C: observed scattering curve (including both scattering in and scattering out), D: the difference between B and C, representing the scattering in signal which is proportional to the differential cross section.

length of the atom beam through the scattering region, V the atom velocity, and e the electronic charge. The upper limit y_{\max}' is the atom displacement for a scattering event in which the electron is scattered through an angle π .

The relation between the probability that an atom is scattered into a range dy' at y' and the probability that the scattered electron is scattered into the range $d\theta$ at θ is

$$p(y')dy' = 2\pi\sigma(\theta) \sin\theta d\theta j_e a / V e,$$

where we have assumed that all azimuthal electron scattering angles at a given θ correspond to the same atomic deflection y' . This assumption introduces an error whose maximum value can be shown¹³ to be $2mv/MV$, where mv and MV are the electronic and atomic momenta, respectively. This error amounts to a maximum of about 3% in the worst cases of the present work. Using the same assumption, the relation between y' and θ is

$$\frac{y'}{d} = \frac{mv}{MV} (1 - \cos\theta), \quad (2)$$

where d is the distance between the scattering region and the detector. In obtaining Eq. (2) it is also assumed that the magnitudes of the electronic and atomic velocities are unchanged by the scattering event. The maximum error introduced by this assumption is also $2mv/MV$. Thus

$$p(y') = \frac{MV}{mv} \frac{2\pi j_e a}{Ve} \frac{\sigma(\theta)}{d}. \quad (3)$$

Curve *D* of Fig. 12 can be used in the following manner to obtain $p(y')$. The total number of atoms $s(y)dy$ scattered per second into a detector of width dy is

¹³ Rubin, Perel, and Bederson, New York University Technical Report No. 1, Nonr 285(15), 1957 (unpublished).

given by

$$s(y)dy = \int_0^y I_{dc}(x)dx p(y-x)dy, \quad (4)$$

where $x < y$ and curve D yields $s(y)$ directly. The quantity $I_{dc}(x)dx$ is the total number of atoms arriving per second in the range dx at x . An iterative procedure could, in principle, now be used to extract values of $p(y')$.

The chief difficulty in applying the above procedure arises from the necessity of an accurate knowledge of the ratio of the scattering out curve to the dc curve. Rather than make an absolute determination of this quantity, a somewhat simpler though less accurate method has been employed. It can be assumed that the scattering in signal at points somewhat to the left of the beam axis can be neglected. This is a reasonable assumption since the scattering in at any point is essentially proportional to the total amount of dc beam to the left of that point. This quantity is small for points near the left edge of the dc beam ($y=0$). Thus the ratio of curves C to A at a point close to $y=0$ is taken as the constant multiplying factor to obtain the scattering out curves from the dc curves. The quantity $p(y')dy'$ is obtained by taking the difference $C-B$ at y' and dividing by the total area under curve A between 0 and the point y' . This gives a value of $p(y')$ which is an average over the range 0 to y' . Equation (3) is now used to obtain $\sigma(\theta)$.

An additional error in the procedure for obtaining $\sigma(\theta)$ arises from the small scattering signal to the left of the dc beam (see Figs. 7 and 8). This signal represents backward scattering, and is due to the action of the magnetic field in the scattering region. This field causes the electrons to follow helical trajectories. Electrons therefore strike the atom beam in a range of angles centering about 90° with respect to the atom beam axis, with the range depending upon the electron energy. Electrons which do not strike the beam at 90° will scatter some atoms to the left of center. The effect is particularly significant at low energies, since the deviation from 90° is determined by the ratio of the forward to the transverse components of the electron velocity. The transverse component is due to the thermal velocity spread, while the forward component is due to the applied voltage. Assuming a thermal spread of 0.50 volt for a cathode at 1000°K , the maximum deviation from 90° of a 2-volt electron beam is about 15° .

The curves for $\sigma(\theta)$ obtained in the above manner for various electron energies are plotted in Fig. 12. In all except the 9-volt curve, the data plotted represent only elastic scattering. This is so because an inelastic scattering event transfers a momentum to the scattered atom which is never less than a minimum amount.⁴ For energies less than 5 eV, the scattering angles corresponding to the minima are greater than the largest

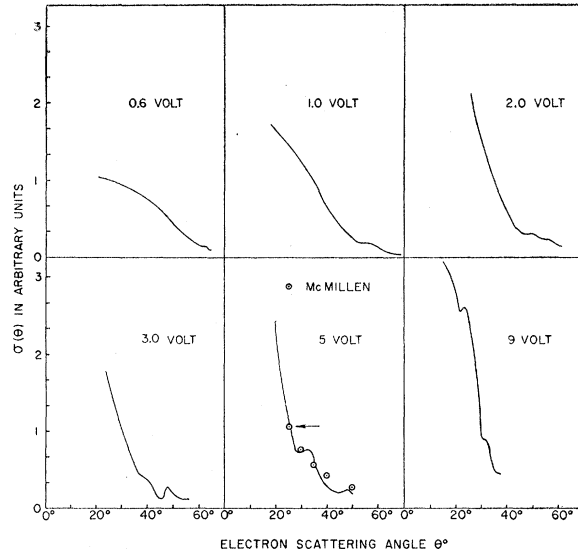


FIG. 12. Differential cross sections $\sigma(\theta)$, as a function of the electron scattering angle θ for electron energies of 0.6, 1.0, 2.0, 3.0, 5.0, and 9.0 volts.

angles studied. Figure 12 also includes some experimental points obtained by McMILLEN.¹⁴ The point marked with an arrow has been normalized to our curve.

In the 9-volt case, $ka \approx 13$, where k is the wave number and a the effective scattering radius of the potassium atom at nine volts. This curve is in surprising agreement with a hard sphere calculation for $\sigma(\theta)$ of Massey and Mohr¹⁵ for a ka of 20. It should be pointed out, however, that above 20° , the experimental data include some contribution due to inelastic scattering.

(b) Exchange Data

The exchange data are tabulated in terms of the ratio of the two polarization peaks, and from these ratios we wish to calculate the fraction of the scattering signal at a given ψ which is due to exchange events. If the atom beam were 100% polarized, and there were no mechanism other than exchange that could cause a change in spin orientation of the atom, we could conclude that the appearance of the second polarization peak is entirely due to exchange events. However, the fact that the beam is not 100% polarized must be taken into account. Furthermore, we can only analyze data taken at points at which we are sure that the scattering is elastic, since for inelastic scattering spin-orbit coupling in the excited state can result in a change in spin orientation when the atom returns to its ground state. For this reason we exclude data taken at detector positions at which some of the scattering may be inelastic.

¹⁴ J. H. McMILLEN, Phys. Rev. **46**, 983 (1934).

¹⁵ H. S. W. Massey and C. B. O. Mohr, Proc. Roy. Soc. (London) **A141**, 434 (1933).

A discussion of the method used to extract values of $\sigma_e(\theta)/\sigma(\theta)$ from the exchange data is given in Appendix I. It is shown there that this ratio is given by

$$\sigma_e(\theta)/\sigma(\theta) = 2/[1 + (R-f)/(1-Rf)],$$

where $R(\psi)$ is the observed ratio of the two polarization peaks at the angle ψ and f is the fraction of the dc beam that possesses the unwanted polarization. In Column IV of Table I, $\sigma_e(\theta)/\sigma(\theta)$ has been tabulated for all the exchange data corresponding to elastic scattering. The value of f was taken to be 0.1. In Column V of Table I, we have listed the total scattering signal in arbitrary units, at each ψ at which exchange data were taken. Column VI, the product of Columns IV and V, gives the exchange signal at ψ in the same arbitrary units as Column V. Notice that the total signal varies more rapidly with angle than the exchange signal. This behavior can also be observed in the two curves shown in Fig. 10. Column VII of Table I gives an estimate, at each energy, of

$$\int_{\theta_{\min}}^{\theta_{\max}} \sigma_e(\theta) d\theta / \int_{\theta_{\min}}^{\theta_{\max}} \sigma(\theta) d\theta,$$

where θ_{\min} and θ_{\max} are the smallest and largest angles at which exchange data were taken. In the low-energy region, this ratio is about 0.3 and appears to be insensitive to the energy.

Lower and upper bounds on the ratio Q_e/Q are tabulated in Columns VIII and IX of Table I, respectively. The lower bounds are obtained by assuming that less than 50% of all exchange events at a given energy were observed, due to the limited motion of the detector. Since (except in the 0.5-volt case) less than one third of the scattered atoms were collected, this assumption is equivalent to stating that $\sigma_e(\theta)/\sigma(\theta)$ will not decrease by more than two on the average at larger angles. The present data indicate that $\sigma_e(\theta)$ is fairly insensitive to θ , while $\sigma(\theta)$ decreases, on the average, with θ , so that the assumption appears reasonable. The upper bounds are obtained by assuming that $\sigma_e(\theta)$ is independent of θ . These bounds are correct provided $\sigma_e(\theta)$ does not, on the average, increase with θ . There appear to be no theoretical reasons to expect such behavior. Column X lists the lower and upper bounds on Q_e in units of 10^{-14} cm², using Brode's data for the absolute values of Q .

Our estimate of the total exchange signal at 0.5 volt is in reasonable agreement with those of Franken *et al.*³ We estimate the exchange cross section to be within the limits 0.8×10^{-14} cm² $< Q_e < 1.6 \times 10^{-14}$ cm², while they obtain an upper limit $Q_e < 3 \times 10^{-14}$ cm². The

agreement may be even better than it appears, since the Franken result is for thermal electrons, and it is probable that the total cross section in this case will be somewhat larger than at 0.5 volt.

ACKNOWLEDGMENT

The authors wish to thank Professor L. H. Fisher for a critical reading of the manuscript, and Mrs. Paula Siagas for her invaluable assistance during the latter phases of the work.

APPENDIX I

In order to obtain values of $\sigma_e(\theta)/\sigma(\theta)$, we must take into account the facts that the electron beam is unpolarized, and that the atom beam is not 100% polarized. Suppose the dc atom beam consists of two spin orientations which we shall call $+$ and $-$. Let the atom current originally in the $+$ state be A , and the atom current originally in the $-$ state be B . The total atom current I may be written as $I = A^+ + B^-$.

Let $E(\psi)$ be the fraction of the total dc beam which is scattered into ψ per unit ψ with a change of spin state. Since the electron beam is unpolarized, we assume that one-half of the exchange scattered atoms will change spin orientation. Thus $2E$ is the fraction of the dc beam which is exchange scattered. Let $D(\psi)$ be the corresponding fraction of the dc beam which is scattered without a change of spin state, so that $D+E$ represents the total fraction of the dc beam which is scattered at ψ . The ratio $2E/(D+E)$ is the fraction of all scattering events at ψ due to exchange scattering. Thus,

$$2E(\psi)/[D(\psi)+E(\psi)] = \sigma_e(\theta)/\sigma(\theta). \quad (A1)$$

Note that while D may contain an interference term between direct and exchange scattering amplitudes, E is proportional to the absolute value of the exchange scattering amplitude squared.

The scattered atom current at ψ is given by

$$I(\psi) = D(A^+ + B^-) + E(A^- + B^+).$$

The experimentally observed ratio $R(\psi)$ of the $+$ spin states to the $-$ spin states in the scattered beam is therefore

$$R(\psi) = (DA^+ + EB^+)/ (EA^- + DB^-).$$

We now drop the superscripts, and define $f = B/A$, which is the fraction of the dc beam in the unwanted spin state. Using (A1), we obtain

$$\sigma_e(\theta)/\sigma(\theta) = 2/[1 + (R-f)/(1-Rf)]. \quad (A2)$$